Journal of Power Sources 195 (2010) 3041–3045

Contents lists available at ScienceDirect

Journal of Power Sources

journal homepage: www.elsevier.com/locate/jpowsour

Short communication

Preparation of graphene nanosheet/carbon nanotube/polyaniline composite as electrode material for supercapacitors

Jun Yan[a], Tong Wei[a], Zhuangjun Fan[a,*], Weizhong Qian[b], Milin Zhang[a], Xiande Shen[a], Fei Wei[b]

[a] Key Laboratory of Superlight Materials and Surface Technology, Ministry of Education, College of Material Science and Chemical Engineering, Harbin Engineering University, Harbin 150001, China

[b] Beijing Key Laboratory of Green Chemical Reaction Engineering and Technology, Department of Chemical Engineering, Tsinghua University, Beijing 100084, China

ARTICLE INFO

Article history:
Received 10 September 2009
Received in revised form 16 October 2009
Accepted 6 November 2009
Available online 11 November 2009

Keywords:
Graphene nanosheet
Carbon nanotube
Composite electrode
Polyaniline
Supercapacitor

ABSTRACT

Graphene nanosheet/carbon nanotube/polyaniline (GNS/CNT/PANI) composite is synthesized via in situ polymerization. GNS/CNT/PANI composite exhibits the specific capacitance of 1035 F g^{-1} (1 mV s^{-1}) in 6 M of KOH, which is a little lower than GNS/PANI composite (1046 F g^{-1}), but much higher than pure PANI (115 F g^{-1}) and CNT/PANI composite (780 F g^{-1}). Though a small amount of CNTs (1 wt.%) is added into GNS, the cycle stability of GNS/CNT/PANI composite is greatly improved due to the maintenance of highly conductive path as well as mechanical strength of the electrode during doping/dedoping processes. After 1000 cycles, the capacitance decreases only 6% of initial capacitance compared to 52% and 67% for GNS/PANI and CNT/PANI composites.

1. Introduction

Supercapacitors, also called electrochemical capacitors (ECs) or ultracapacitors, have attracted considerable attention over the past decades because of their higher power density and longer cycle life than secondary batteries and their higher energy density compared to conventional electrical double-layer capacitors [1–6]. To develop an advanced supercapacitor device, an active electrode material with high capacity performance is indispensable [2,7]. Recently, many attempts have been devoted to the use of electronically conducting polymers as electrode materials in supercapacitors such as polyaniline (PANI), polypyrrole, poly(ethylenedioxythiophene), polythiophene and its substituted counterparts [1]. The increasing interest in such polymers is stimulated by the demand of electroactive materials with both high power and energy density as well as low fabrication costs [8]. Among these materials, PANI has been considered as one of the most promising electrode materials because of its low cost, easy synthesis and relatively high conductivity and lower cost than many other conducting polymers [8]. However, it exhibits the disadvantage of a low cycle life because swelling and shrinkage may occur during doping/dedoping processes, thus, leading to mechanical degradation of the electrodes and fading of the electrochemical performance [9,10]. The combination of PANI with various porous carbon materials has been proved to be attractive to reinforce the stability of PANI as well as maximize the capacitance value. Gupta et al. reported the electrochemical polymerization of PANI/SWCNT composites with the highest specific capacitance of 463 F g^{-1} obtained for 73 wt.% PANI [11,12], and the highest specific capacitance value of 500 F g^{-1} for the MWCNT/PANI composite film containing MWCNT of 0.8 wt.% [13]. Li et al. prepared ordered mesoporous carbon/PANI composite via in situ polymerization, and the composite exhibited the highest specific capacitance of 747 F g^{-1} at a current density of 0.1 A g^{-1} and excellent rate capability [10]. Jang et al. synthesized PANI coated carbon nanofibers by one-step vapor deposition polymerization technique, and the maximum specific capacitance was 264 F g^{-1} when the thickness of PANI layer was ca. 20 nm [14]. Compared with carbon nanotubes, graphene nanosheets (GNS) are predicted as an excellent support material due to their high surface area, remarkable mechanical stiffness and excellent conductivity [15].

Herein, we reported a simple process to synthesis the composite of GNS/CNT/PANI via in situ polymerization. The introduction of 1 wt.% CNTs could greatly improve the long-term cycle stability of GNS/CNT/PANI composite. The morphology, microstructure and electrochemical performances of the resultant composites were investigated, and the effect of CNTs on the electrochemical performance was also studied.

* Corresponding author. Tel.: +86 451 82569890; fax: +86 451 82569890.
E-mail address: fanzhj666@163.com (Z. Fan).

0378-7753/$ – see front matter © 2009 Elsevier B.V. All rights reserved.
doi:10.1016/j.jpowsour.2009.11.028

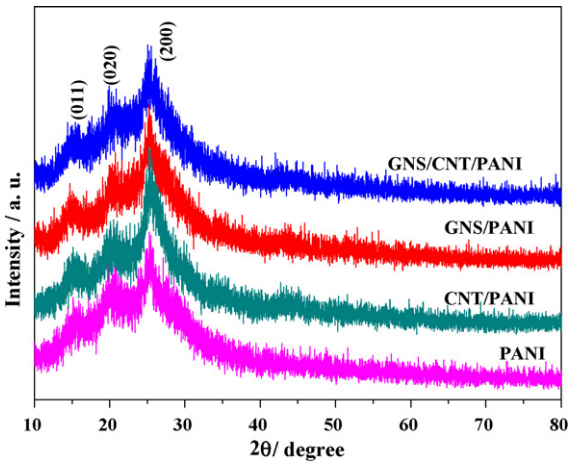

Fig. 1. Typical XRD patterns of the as-prepared PANI, CNT/PANI, GNS/PANI and GNS/CNT/PANI samples.

2. Experimental

2.1. Synthesis of GNS/CNT/PANI composites

All the chemicals were of analytical grade and were used without further purification. CNTs were prepared from the decomposition of hydrocarbons over $Fe/Mo/Al_2O_3$ catalyst using a fluidization method and have average outer diameter of 20–30 nm [16,17], and then refluxed in a mixture (3:1, v/v) of concentrated sulfuric (98 wt.%) and nitric acids (65 wt.%) for 2 h to remove the catalyst particles and other impurities. GNS was prepared by reduction of graphite oxide with hydrazine hydrate as described elsewhere [18]. 0.165 g GNS and CNTs (mass ratio of GNS to CNTs is 99:1) were added into 135 mL of H_2O and sonicated for 2 h. Then 0.25 M aniline monomers (40 mL, solvent: 1 M HCl) were added into GNS/CNT suspension and sonicated for 30 min. Afterwards, an equal volume of 0.25 M ammonium persulfate (APS) solution was added into the above mixture and kept at 0–4 °C for 4 h. Finally, GNS/CNT/PANI composite was washed with distilled water and ethanol, dried in a vacuum oven at 80 °C for 12 h. The mass fraction of PANI calculated from the weight of GNS before and after polymerization was 85%. For comparison, CNT/PANI and GNS/PANI were also prepared through the above-mentioned chemical process.

2.2. Characterization methods

The crystallographic structures of the materials were determined by a powder X-ray diffraction system (XRD, TTR-III) equipped with Cu Kα radiation (λ = 0.15406 nm). The microstructure of the samples was investigated by a scanning electron microscopy (SEM, Camscan Mx2600FE) and transition electron microscopy (TEM, JEOL JEM2010).

2.3. Preparation of electrodes and electrochemical measurement

The fabrication of working electrodes was carried out as described elsewhere [19]. Briefly, the electroactive materials, carbon black and poly(tetrafluoroethylene) (PTFE) were mixed in a mass ratio of 75:20:5 and dispersed in ethanol. Then the resulting mixture was coated onto the nickel foam substrate (1 cm × 1 cm) with a spatula, which was followed by drying at 100 °C for 12 h in a

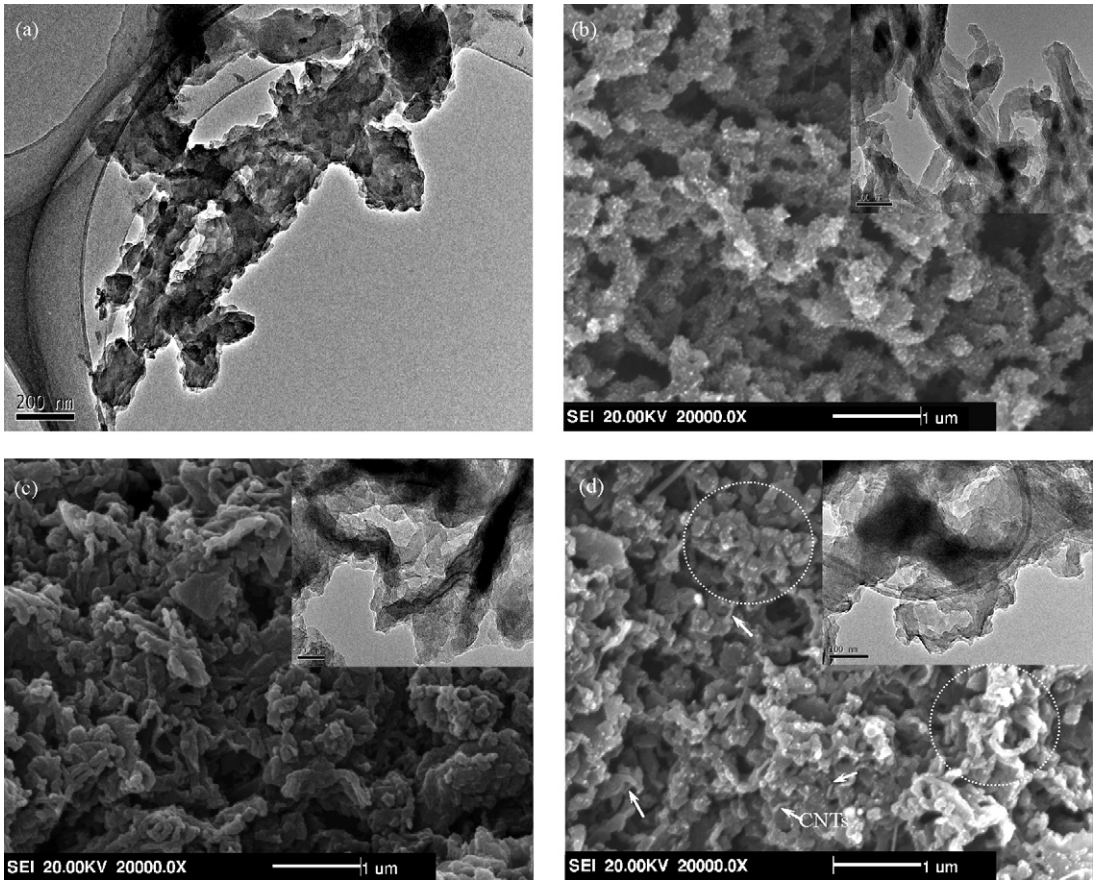

Fig. 2. (a) TEM image of pure PANI and (b–d) SEM images of CNT/PANI, GNS/PANI and GNS/CNT/PANI composite (inset exhibits the corresponding TEM images).

vacuum oven. The mass of each electrode was about 4 mg, including conducting agent and binder.

All electrochemical measurements were done in a three-electrode setup: Ni foam coated with composites as the working electrode, platinum foil and Hg/HgO electrode as the counter and reference electrodes. The measurements were carried out in a 6 M KOH aqueous electrolyte at room temperature. Cyclic voltammetry (CV), galvanostatic charge/discharge and electrochemical impedance spectroscopy (EIS) were measured by a CHI 660C electrochemical workstation. CV tests were done between −0.7 and 0.3 V (vs. Hg/HgO) at different scan rates of 1, 10, 20, 50, 100, 200 and 500 mV s^{-1}. Galvanostatic charge/discharge curves were measured at different current densities of 2, 10, 20 and 50 mA cm^{-2}, and EIS measurements were also carried out in the frequency range from 100 kHz to 0.1 Hz at open circuit potential with an ac perturbation of 5 mV.

3. Results and discussion

3.1. Microstructure characterizations

Fig. 1 shows the XRD patterns of pure PANI, CNT/PANI, GNS/PANI and GNS/CNTs/PANI composites. For pure PANI, the crystalline peaks appear at $2\theta = 15.3^\circ$, 20.7° and 25.2°, corresponding to (0 1 1), (0 2 0) and (2 0 0) crystal planes of PANI in its emeraldine salt form, respectively [20]. The X-ray data of the three composites presents crystalline peaks similar to those obtained from pure PANI, revealing that no additional crystalline order has been introduced into the composites.

Fig. 2 shows the SEM and TEM images of as-prepared samples. During polymerization without GNS and/or CNTs, PANI particles (about 40 nm) form rod-like agglomerations with ~170 nm in diameter and 1–2 μm in length (Fig. 2a). Once doped with CNTs, the PANI particles homogeneously coat on the surfaces of CNTs with thickness of ~20 nm (Fig. 2b), and some PANI agglomerates (25–40 nm) are also observed on outside of CNTs (Fig. 2b, inset). As for GNS/PANI composite, PANI particles with the size of ~2 nm coat on the surfaces of GNS (marked by arrows in Fig. 2c). If added 1 wt.% CNTs into GNS, PANI particles preferentially grow on the surfaces of GNS due to their high chemical activity and surface area [21], and the surfaces of CNTs are rather smooth (Fig. 2d, inset). Compared with GNS/PANI composite, there are more PANI agglomerations in GNS/CNT/PANI composite (marked by circles in Fig. 2d). GNS are used as support materials for deposition of PANI particles and CNTs as conductive wires interconnected among GNS/PANI particles, such structure would be beneficent to further improve the conductivity of the composite.

3.2. Electrochemical behavior

The specific capacitance of the electrode can be calculated according to the following equation:

$$C = \frac{\int IdV}{\upsilon m V} \quad (1)$$

where I is the response current density (A cm^{-2}), V is the potential (V), υ is the potential scan rate (V s^{-1}), and m is the mass of the electroactive materials (as-prepared composites) in the electrodes (g).

Fig. 3 shows the CV curves of as-prepared samples, where the current has been transferred into the specific current per unit mass of electroactive material. Positive currents in the figures are for oxidation and the negative currents are for reduction processes. In Fig. 3a, it can be found that there are a couple of redox peaks in CV curves of pure PANI and the as-prepared composites, attributed to

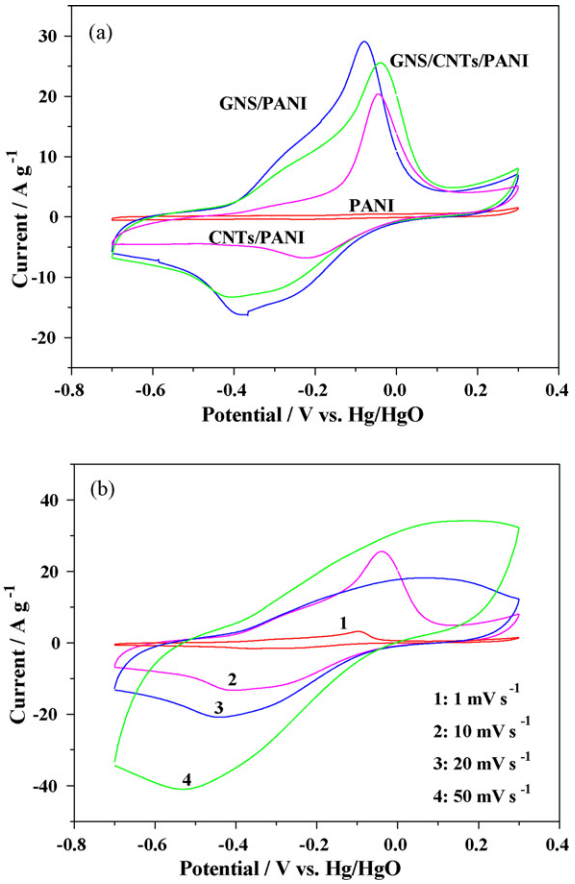

Fig. 3. (a) CV curves of pure PANI, CNT/PANI, GNS/PANI and GNS/CNT/PANI composite at 10 mV s^{-1}, and (b) CV curves of GNS/CNT/PANI composite at different scan rates of 1, 10, 20 and 50 mV s^{-1}, where the current has been transferred into the specific current per unit mass of electroactive material.

the redox transition of PANI between a semiconducting state (leucoemeraldine form) and a conducting sate (polaronic emeraldine form) [8], which results in the redox capacitance. The differences between the oxidation and reduction peaks, $\Delta E_{O,R}$, is taken as an estimate of the reversibility of the redox reaction [22]. Values of 0.18, 0.29 and 0.37 V are obtained for the redox reactions of PANI with GNS and/or CNTs incorporation, compared to 0.48 V for pure PANI, indicating that the redox reactions appear to occur more reversibly after the addition of GNS and/or CNTs. In addition, the larger current density response of GNS/PANI composite electrode means higher specific capacitance than that of pure PANI, CNT/PANI and GNS/CNT/PANI composites. The dispersion of nanoscale PANI particles on GNS reduces the diffusion and migration length of the electrolyte ions during the fast charge/discharge process and increases the electrochemical utilization of PANI. Fig. 3b shows CV curves of GNS/CNT/PANI composite at different scan rates. It can be noted that the cathodic peaks shift positively and the anodic peaks shift negatively with the increase of potential scan rates from 1 to 50 mV s^{-1}, which is mainly due to the resistance of the electrode [8]. Furthermore, the obvious increase of current with scan rates means a good rate capability for GNS/CNT/PANI composite electrode.

Fig. 4 shows the galvanostatic charge/discharge curves of the pure PANI and as-prepared composites. From Fig. 4a, it can be noted that the charge voltage becomes lower and the discharge voltage becomes higher after GNS and/or CNTs are incorporated in the PANI. This indicates that the energy consumed by the internal resistance is reduced and, therefore, the effective energy storage is improved. This improvement is perhaps due to the fact that the inner resistance of the electrode is reduced when GNS

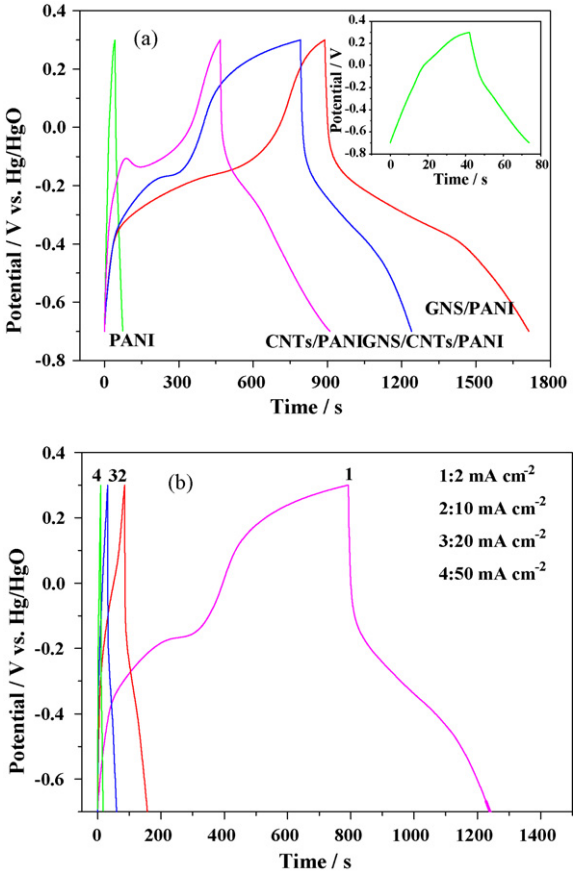

Fig. 4. (a) Galvanostatic charge/discharge tests of pure PANI and as-prepared composites at 2 mA cm^{-2}. (b) Galvanostatic charge/discharge tests of GNS/CNT/PANI composite at different current densities of 2, 10, 20 and 50 mA cm^{-2}.

and/or CNTs are present. In Fig. 4b, the charge/discharge duration of GNS/CNT/PANI composite decreases with the current densities from 1 to 50 mA cm^{-2}. It can be seen obviously that there are two clear voltage stages included in the curves: −0.2 to 0.3 and −0.7 to −0.2 V, respectively. During the former, short charge/discharge duration is ascribed purely to the electric double-layer capacitance of the electrode. During the latter, the combination of electric double-layer capacitance and Faradaic capacitance is responsible for the longer charge/discharge duration due to Faradaic charge-transfer accompanied by the double-layer charging/discharging process. These results are in accordance with those deduced from the CV tests.

Fig. 5 shows the variation in the specific capacitance of pure PANI and as-prepared composites as a function of scan rates. It can be observed that the specific capacitance of GNS/CNT/PANI is much higher than that of pure PANI and CNT/PANI composite but lower than that of GNS/PANI composite at the same scan rates. The maximum specific capacitance of 1035 F g^{-1} is obtained at a scan rate of 1 mV s^{-1} for GNS/CNT/PANI composite compared to 115, 780 and 1046 F g^{-1} for pure PANI, CNT/PANI and GNS/PANI, respectively. The greatly enhanced specific capacitance is due to the synergistic effect between GNS and PANI [8]. In addition, the small nanometer-sized PANI can exhibit enhanced electrode/electrolyte interface areas, providing high electroactive regions and short diffusion lengths [23], which can ensure the high utilization of PANI. For GNS/CNT/PANI composite, more PANI agglomerations are observed than that of GNS/PANI, resulting low electrochemical utilization of PANI (Fig. 2d). What is more, the specific capacitance of GNS/CNT/PANI composite is much larger than that of SWCNT/PANI (350–485 F g^{-1}) [11,12,24], porous carbon/PANI (160–180 F g^{-1}) [25,26], MWCNT/PANI (322–606 F g^{-1}) [27,28], activated carbon/PANI (380–500 F g^{-1}) [29,30], ordered mesoporous carbon/PANI (747–900 F g^{-1}) [8,10] and carbon nanofiber/PANI (264 F g^{-1}) [14].

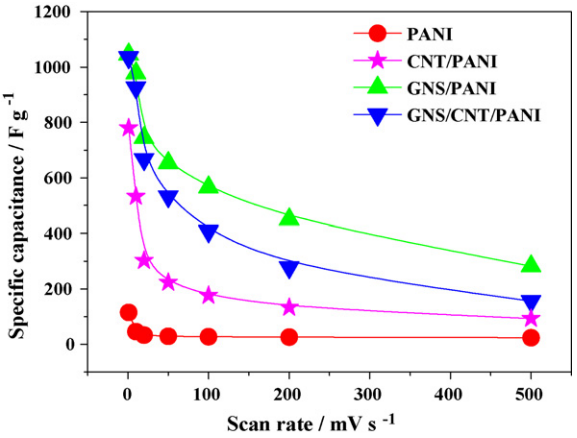

Fig. 5. Specific capacitance of PANI and PANI based composites at different scan rates.

The long-term cycle stability of the GNS/PANI, CNT/PANI and GNS/CNT/PANI composites was also evaluated in this study by repeating the CV test between −0.7 and 0.3 V (vs. Hg/HgO) at a scan rate of 200 mV s^{-1} for 1000 cycles. The specific capacitance based on electroactive materials as a function of cycle number is presented in Fig. 6. The GNS/CNT/PANI electrode is found to exhibit excellent stability over the entire cycle numbers. After the first cycle, the specific capacitance increases by 11% and the electrode thereafter reaches the stability state. After 1000 cycles, the capacitance decreases only 6% of initial capacitance compared to 52% and 67% for GNS/PANI and CNT/PANI composites demonstrating that GNS/CNT/PANI electrode exhibits excellent cycle stability. The decrease of specific capacitance could be attributed to the swelling and shrinkage during the long-term charge/discharge processes [31]. PANI particles on GNS could interconnect with each other provided by CNT conductive network as well as the improvement of mechanical strength (Fig. 7). Therefore, this unique structure is favorable for the enhanced of the electrochemical performance.

Impedance of the GNS/CNT/PANI composite after the 1st and 1000th cycle was measured in the frequency range of 100 kHz to 0.1 Hz at open circuit potential with an ac perturbation of 5 mV (Fig. 8). It could be obviously seen that the impedance spectra

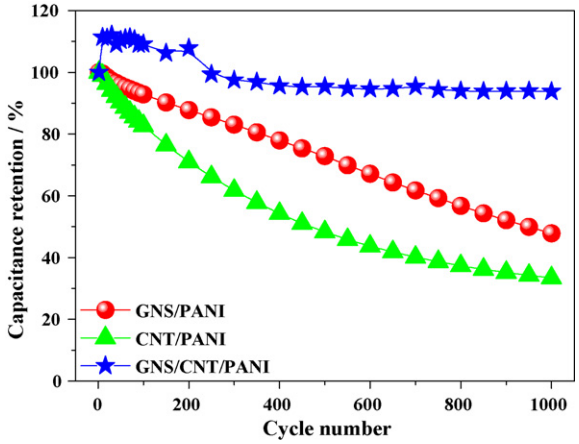

Fig. 6. Variation of the specific capacitance of PANI based composites as a function of cycle number measured at 200 mV s^{-1} in 6 M KOH aqueous solution.

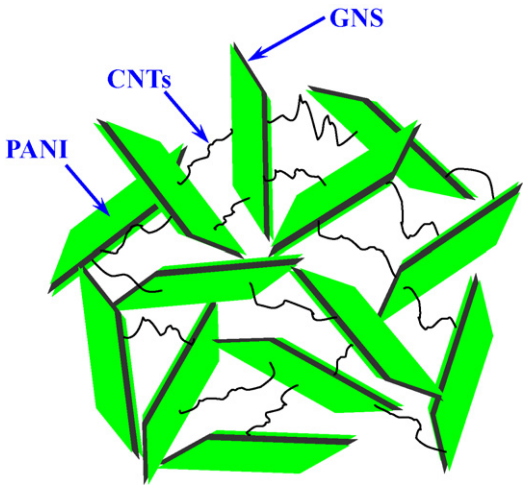

Fig. 7. Schematic illustration of the effect of CNTs on electrochemical performance of the GNS/CNT/PANI composite.

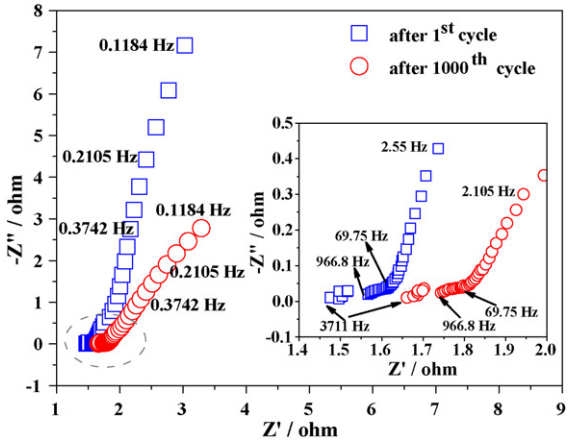

Fig. 8. Nyquist plots of GNS/CNT/PANI electrode in the frequency range of 100 kHz to 0.1 Hz measured during the cycle life testing (inset is the enlargement of dashed segment, representing the high-frequency region).

are almost similar in form, composed of one semicircle at high-frequency end followed by a linear part at the low-frequency end. After 1000th cycle, the internal resistance increases from 1.48 to 1.66 Ω and the diffusion limitation is also enhanced, which is probably attributable to the composite crack during charge/discharge and then part of the PANI deposits loses contact with each other due to the swelling and shrinkage.

4. Conclusions

In this paper, GNS/CNT/PANI composite was synthesized via in situ polymerization. GNS are used as support materials for deposition of PANI particles and CNTs as conductive wires interconnected among GNS/PANI particles. CNTs can not only provide highly conductive path resulting in the improvement of conductivity of composite, but also maintain the mechanical strength. The maximum specific capacitance is 1035 $F g^{-1}$ at a scan rate of 1 $mV s^{-1}$ in 6 M KOH. After 1000 cycles, the capacitance decreases only 6% of initial capacitance compared to 52% and 67% for GNS/PANI and CNT/PANI composites demonstrating that GNS/CNT/PANI electrode has excellent cycle stability. Therefore, the intriguing GNS/CNT/PANI composite is quite a suitable and promising electrode material for supercapacitors.

Acknowledgements

This work was supported by the Key Project of Chinese Ministry of Education (No. 106011), Foundation of Harbin Innovation Fellow (2006RFQXG030 and 2007RFQXG028) and Fundamental Research Foundation of Harbin Engineering University (Project HEUFT07094).

References

[1] B.E. Conway, Electrochemical Supercapacitors: Scientific Fundamentals and Technological Applications, Kluwer Academic/Plenum Publishers, New York, 1999.
[2] G.-W. Yang, C.-L. Xu, H.-L. Li, Chem. Commun. 48 (2008) 6537.
[3] P. Simon, Y. Gogotsi, Nat. Mater. 7 (2008) 845.
[4] J.-K. Chang, C.-H. Huang, W.-T. Tsai, M.-J. Deng, I.W. Sun, J. Power Sources 179 (2008) 435.
[5] G. An, P. Yu, M. Xiao, Z. Liu, Z. Miao, K. Ding, L. Mao, Nanotechnology 19 (2008) 275709.
[6] D.W. Liu, Q.F. Zhang, P. Xiao, B.B. Garcia, Q. Guo, R. Champion, G.Z. Cao, Chem. Mater. 20 (2008) 1376.
[7] C.-C. Hu, K.-H. Chang, M.-C. Lin, Y.-T. Wu, Nano Lett. 6 (2006) 2690.
[8] Y.G. Wang, H.Q. Li, Y.Y. Xia, Adv. Mater. 18 (2006) 2619.
[9] L.Z. Fan, Y.S. Hu, J. Maier, P. Adelhelm, B. Smarsly, M. Antonietti, Adv. Funct. Mater. 17 (2007) 3083.
[10] L.X. Li, H.H. Song, Q.C. Zhang, J.Y. Yao, X.H. Chen, J. Power Sources 187 (2009) 268.
[11] V. Gupta, N. Miura, Electrochim. Acta 52 (2005) 1721.
[12] V. Gupta, N. Miura, J. Power Sources 157 (2006) 616.
[13] J. Zhang, L.B. Kong, B. Wang, Y.C. Luo, L. Kang, Synth. Met. 159 (2009) 260.
[14] J. Jang, J. Bae, M. Choi, S.H. Yoon, Carbon 43 (2005) 2730.
[15] S. Stankovich, D.A. Dikin, G.H.B. Dommett, K.M. Kohlhaas, E.J. Zimney, E.A. Stach, R.D. Piner, S.T. Nguyen, R.S. Ruoff, Nature 442 (2006) 282.
[16] Y. Wang, F. Wei, G.H. Luo, H. Yu, G.S. Gu, Chem. Phys. Lett. 364 (2002) 568.
[17] W.Z. Qian, H. Yu, F. Wei, Q.F. Zhang, Z.W. Wang, Carbon 40 (2002) 2968.
[18] S. Stankovich, D.A. Dikin, R.D. Piner, K.A. Kohlhaas, A. Kleinhammes, Y. Jia, Y. Wu, S.T. Nguyen, R.S. Ruoff, Carbon 45 (2007) 1558.
[19] J. Yan, Z. Fan, T. Wei, J. Cheng, B. Shao, K. Wang, L. Song, M. Zhang, J. Power Sources 194 (2009) 1202.
[20] H.K. Chaudhari, D.S. Kelkar, Polym. Int. 42 (1997) 380.
[21] S.M. Paek, E. Yoo, I. Honma, Nano Lett. 9 (2009) 72.
[22] C.Y. Wang, V. Mottaghitalab, C.O. Too, G.M. Spinks, G.G. Wallace, J. Power Sources 163 (2007) 1105.
[23] H. Zhang, G.P. Cao, W.K. Wang, K.G. Yuan, B. Xu, W.F. Zhang, J. Cheng, Y.S. Yang, Electrochim. Acta 54 (2009) 1153.
[24] Y.K. Zhou, B.L. He, W.J. Zhou, H.L. Li, J. Electrochem. Soc. 151 (2004) A1052.
[25] W.C. Chen, T.C. Wen, J. Power Sources 117 (2003) 273.
[26] W.C. Chen, T.C. Wen, H.S. Teng, Electrochim. Acta 48 (2003) 641.
[27] S.R. Sivakkumar, W.J. Kim, J.A. Choi, D.R. MacFarlane, M. Forsyth, D.W. Kim, J. Power Sources 171 (2007) 1062.
[28] H.Y. Mi, X.G. Zhang, S.Y. An, X.G. Ye, S.D. Yang, Electrochem. Commun. 9 (2007) 2859.
[29] J.H. Park, O.O. Park, J. Power Sources 111 (2002) 185.
[30] M.J. Bleda-Martinez, C. Peng, S.G. Zhang, G.Z. Chen, E. Morallon, D. Cazorla-Amoros, J. Electrochem. Soc. 155 (2008) A672.
[31] V. Khomenko, E. Frackowiak, F. Beguin, Electrochim. Acta 50 (2005) 2499.